Joint Pathology Center
Veterinary Pathology Services

WEDNESDAY SLIDE CONFERENCE 2021-2022

C o n f e r e n c e 17

2 February 2022

CASE I: Case 2 (JPC 4118311)

Signalment:
Approximately 5 year-old, intact, female, Indian-origin, rhesus macaque (*Macaca mulatta)*

History:
This macaque was humanely euthanized after reaching experimental endpoint criteria 8 days following intramuscular challenge with a viral agent.

Gross Pathology:
Body as a whole: Good body condition with moderate dehydration
Liver: Severe, subacute, diffuse hepatic necrosis and lipidosis with severe hepatomegaly
Spleen: Moderate, subacute, diffuse necrotizing splenomegaly (fibrinoid necrosis)
Kidneys: Severe, subacute, diffuse renomegaly (congestion and edema)
Lung: Mild, acute, multifocal hemorrhage
Tracheobronchial lymph nodes: Moderate, subacute, diffuse lymphadenopathy
Peripheral and mesenteric lymph nodes: Moderate, subacute, diffuse lymphadenopathy
Adrenal glands: Subacute, moderate, diffuse congestion
Skin covering the chest: Subacute, locally extensive, mild petechial hemorrhage
Dorsal skin of the neck: Subacute, focal, mild ecchymotic hemorrhage
Stomach: Mild, acute gas distention

Laboratory Results:
See Tables 1 and 2

Pre- & Post- Challenge Day	WBC $x10^3/\mu L$	Neutrophils $x10^3/\mu L$	Lymphocytes $x10^3/\mu L$	Monocytes $x10^3/\mu L$	Platelets $x10^9/\mu L$
-14	6.65	3.31	2.78	0.47	311
-7	6.14	2.97	2.62	0.44	328
0	6.07	2.84	2.75	0.42	371
3	6.60	5.24	1.12	0.24	313
6	5.22	4.08	0.98	0.16	252
8	8.90	3.36	4.63	0.56	379
Normal Range	6.4	3.5	1.6	0	313
	10.2	5.8	5.1	0.4	475

Table 1

Pre- & Post-Challenge Day	Albumin g/dL	Total Protein g/dL	ALT U/L	AST U/L	GGT U/L	BUN mg/dL	Creatinine mg/dL
-14	3.5	7.0	40	28	53	22	0.6
-7	3.5	6.5	52	22	52	16	0.6
0	3.6	7.3	61	33	58	19	0.7
3	3.8	6.7	68	37	55	21	0.9
6	3.4	6.2	443	1,098	219	-	1.1
8	2.5	5.2	1,244	ND	321	34	3.8
Normal Range	3.2	5.9	26	24	48	16	0.8
	4.1	7.9	52	38	76	22	1.2

Table 2

Ultrastructural Description:
The image contains degenerate organellar cellular debris, variably electron-dense amorphous material (protein), two degenerate cells, approximately 25 single-cell organisms, and myriad filamentous viral particles. The electron-dense, single-cell organisms are round, measure 0.8-1 micron, lack a nucleus, and have a prominent bi-layer cell membrane that is electron lucent centrally. These organisms are sometimes arranged in pairs (diplococci). The filamentous viral particles measure approximately 80 nm in diameter and, within the image, up to 800 nm in length. The viral nucleocapsids are electron-dense with a striated core and surrounded by a viral envelope. The free ends of occasional virus particles fold back onto themselves forming a hook- or loop-like structure multifocally. The two partially intact cells within the image are polygonal, with indistinct, organellar and cellular membranes. The nuclei in these cells are markedly swollen and moderately electron dense with fragmented, dispersed, electron-dense chromatin. Viral particles are present adjacent to the nuclear membrane, but it cannot be definitively discerned if these are intracytoplasmic viral particles. A medium electron-dense, 1.5x1 micron, aggregate of proteinaceous material (viral nucleocapsids) formed by 20-25 nm tightly-arranged tubules is present in the upper left-hand side of the image (viral inclusion body). Adjacent to this inclusion body are approximately ten, 300-500 nm, elongated clusters of electron-dense material composed of thousands of compact filaments (fibrin).

Contributor's Morphologic Diagnoses:
Tissue: Severe, diffuse, fibrinous necrosis with intralesional myriad filamentous viral particles and multifocal diplococcal bacteria

Contributor's Comment:
The tissue composing the TEM images cannot be discerned. The images are from the

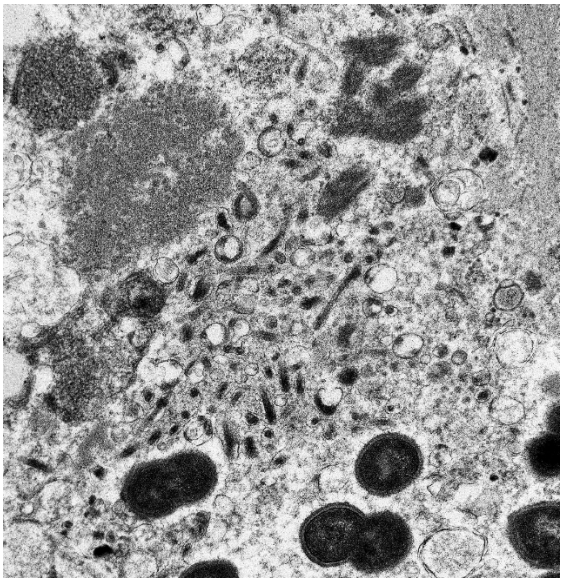

Figure 1-1. Indeterminate tissue, rhesus macaque: This electron micrograph demonstrates numerous linear to curled viral particles (center) as well as aggregates of homogenous and tubular viral proteins. (21,000X)

spleen of a five-year-old, intact, female macaque inoculated with Marburg virus (MARV) intramuscularly 8 days prior to euthanasia. Histologically, the normal architecture of the spleen was effaced by necrosis and bacterial colonies were numerous. Bacterial emboli were also seen in the inoculation site musculature, peripheral and visceral lymph nodes, liver, stomach, small intestine, adrenal glands, bladder, bone marrow, and brain. Bacteria commonly recognized to form diplococci include Gram positive cocci - *Streptococcus pneumoniae* and *Enterococcus* spp.; and gram-negative cocci: *Neisseria* spp., *Moraxella catarrhalis*, and *Acinetobacter* spp. The bacterial septicemia observed in this macaque histologically is thought to be peracute, as there is no clinical pathological evidence of a response to the bacteria in blood samples collected immediately prior to necropsy or in the tissues collected at necropsy. The bacteria seen in this case are thought to be *Streptococcus pneumoniae* but additional diagnostics were not performed to identify the bacteria in this case.

The gross, clinical pathologic, and histopathologic lesions seen in this macaque are consistent with those seen in the macaque model of MARV disease.[5,8] Pathogenic filoviruses include Ebola virus (*Zaire ebolavirus, Sudan ebolavirus, Tai Forest ebolavirus, Bundibugyo ebolavirus*) and Marburg virus.[7] Reston virus (*Reston ebolavirus*) is only known to cause disease in primates and pigs; seropositivity alone has been observed in humans following occupational exposure.[7] Following exposure, MARV infects, replicates, and disseminates throughout the body in monocytes and macrophages.[1] The marked elevations in ALT, AST, and GGT seen in this macaque reflect direct infection and destruction of hepatocytes by MARV.[8] The azotemia observed clinically is pre-renal though terminal thrombosis of the renal vasculature due to the coagulopathy induced by MARV is commonly seen.[11] Hypoproteinemia is almost universally seen in MARV-infected macaques and thought to be secondary to both hepatic dysfunction and protein loss secondary to increased vascular permeability. Lymphocytes are not infected by MARV but a poorly characterized, "bystander" lymphocytolysis is thought to occur after the onset of infection.[4] Widespread lymphoid depletion and necrosis were observed in this macaque terminally, consistent with the modest lymphoid response observed clinicopathologically despite fulminant MARV infection.

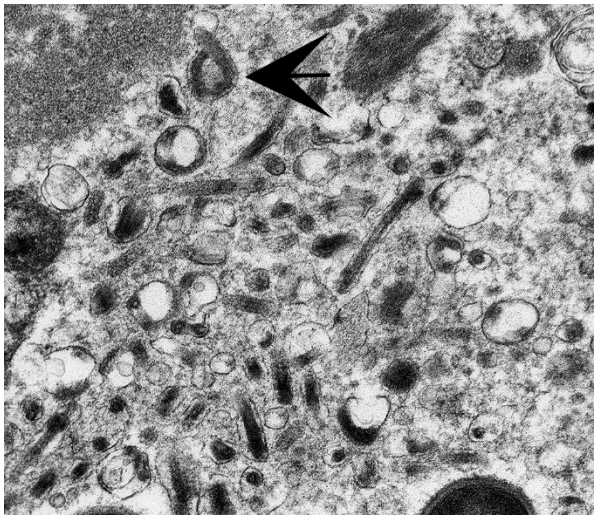

Figure 1-2. Indeterminate tissue, rhesus macaque: Filovirus particles are free in the cytoplasm and one (arrow) curls back upon itself at one end. (21,000X)

Contributing Institution:
Pathology Department
NIH/NIAID
Integrated Research Facility
https://www.niaid.nih.gov/about/integrated-research-facility

JPC Diagnosis:
Undetermined tissue: Cellular degeneration, severe, with intracytoplasmic filoviral particles and cocci.

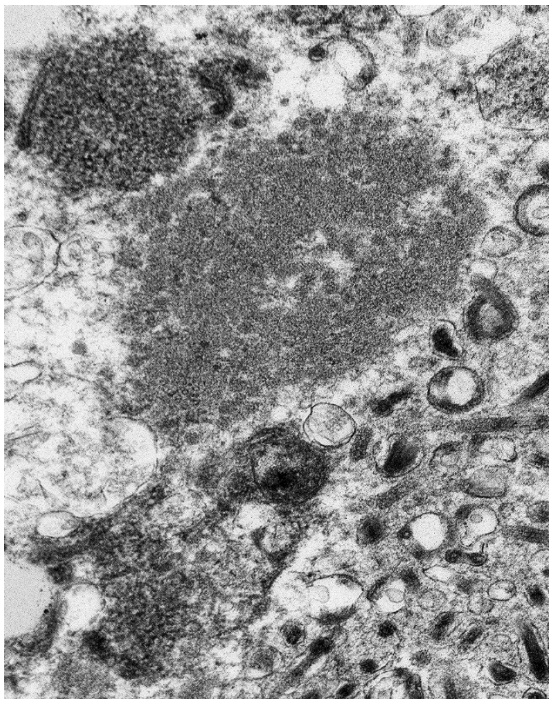

Figure 1-3. Indeterminate tissue, rhesus macaque: There are several intracytoplasmic viral inclusions composed of tubular and homogenous aggregates of viral protein. (21,000X)

JPC Comment:

Viral hemorrhagic fever (VHF) in humans is a syndrome characterized by acute fever with systemic involvement and generalized hemorrhage may occur in severe cases. Viral families associated with VHF include genera of *Arenaviriade* (e.g. Lassa virus), *Bunyaviridae* (e.g. Crimea-Congo hemorrhagic fever, Rift Valley fever, and *Hantavirus*), *Flaviviridae* (e.g. Dengue hemorrhagic fever and yellow fever), and *Filoviridae* as previously described by the contributor. Although HF viruses are diverse in morphology and size, all are single-stranded RNA viruses with a lipid envelope, which makes them vulnerable to detergents, low pH environments, and household bleach. However, these viruses are stable at a neutral pH, especially in the presence of protein. For example, Ebola virus was cultured from desiccated blood found in syringes stored at room temperature for approximately a month during a Central African outbreak in 1995. All HF viruses, with the exception of dengue viruses, are biosafety level (BSL) 3 or 4 agents due to their tendencies to remain stable and infectious as fine particle aerosols and their ability to produce disease with high morbidity and mortality; both Marburg and Ebola virus are BSL-4 agents.[6]

Ebola and Marburg virus particles are very similar. Both contain a 19-kb, single, negative-stranded, linear genome encoding seven structural proteins. Three of these proteins, GP, VP24, and VP40, are associated with the membrane. GP is the effector protein for binding and membrane fusion. Interestingly, the GP gene is distinctly different between the Ebola and the Marburg viruses. The Marburg virus GP gene encodes a single product (GP) in a conventional open reading frame whereas Ebola virus encode the GP in two open reading frames that are expressed through transcriptional editing. VP40 is a matrix protein and is responsible for the formation of the particle's filamentous appearance. VP24 may have a role in viral assembly and budding.[6]

HF viruses exhibit a stereotypical pathogenesis in both humans and non-human primates (NHPs). Following initial infection, the virus spreads to the regional lymph nodes, liver, and spleen where tissue macrophages and dendritic cells are infected, which in turn release cytokines that recruit additional target cells to the site of infection. Although lymphocytes are not directly targeted by the

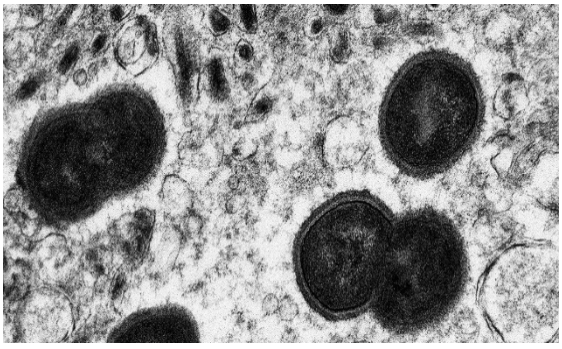

Figure 1-4. Indeterminate tissue, rhesus macaque: Paired cocci are free within the cytoplasm. (21,000X)

virus, marked lymphocytolysis appears to be the most consistent pathological finding amongst HF viral infections of humans and NHPs, with the exception of hantaviruses. The underlying cause of lymphoid depletion is likely multifactorial, including second order effects from dendritic cell infection and the release of soluble factors from virus infected monocytes and macrophages, resulting in decreased lymphocyte survival signals and upregulation of proapoptotic proteins such as Fas and tumor necrosis factor-related apoptosis virus inducing ligand (TRAIL), respectively. Coagulation anomalies vary in regard to both mechanism and severity between the etiologies. For example, Ebola causes overexpression of tissue factor (factor III), resulting in activation of the extrinsic coagulation pathway and the formation intravascular fibrin thrombi. Coagulation and hemodynamic disturbances are common features of HFVs, largely due to hepatocyte and adrenal cortical cell infection. Hepatocellular infection results in impaired synthesis of both coagulation factors and albumin, predisposing to coagulopathy and decreased oncotic pressure, contributing toward both hypotension and edema.

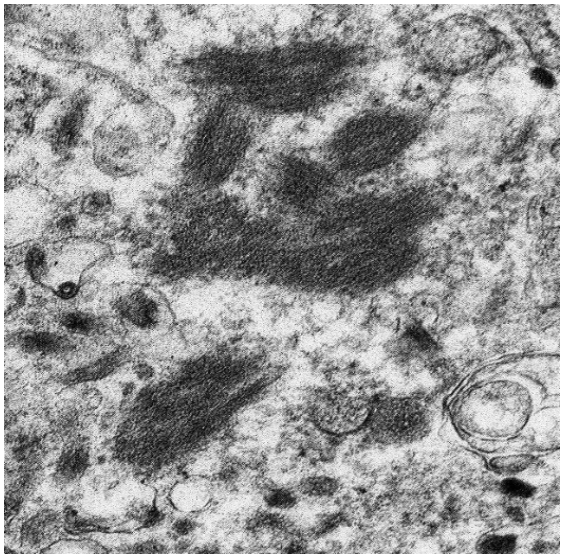

Figure 1-5. Indeterminate tissue, rhesus macaque: Aggregates of fibrin are present within the cystoplasm of this presumed macrophage. (21,000X)

Infection of adrenal cortical cells results in impaired steroid production, resulting in hypotension and sodium loss with hypovolemia.[6]

Most VHF infections in both humans and NHPs are associated with cutaneous flushing or macular rashes with varying characteristics (though with significant crossover) depending on the agent. More than 50% of humans and macaques infected with Marburg virus and Ebola virus develop nonpruritic petechial dermal rashes on the axillae and groin, forehead, and chest. Arenavirus HF in humans and NHPs is associated with flushed erythematous rashes on the face and thorax, though axillary and oral petechiae are also commonly observed in human cases.[6]

Histologically, fibrin and fibrinocellular thrombi in numerous tissues and deposition of fibrin in the splenic red pulp and marginal zones are common findings in infected cynomolgus and rhesus macaques.[6]

As demonstrated by transmission electronic microscopy (TEM) in this case, filoviruses are characterized by their unique filamentous appearance for which they are named (*filum*; Latin for "thread"). Marburg virus was the first of the filoviruses to be discovered, following three geographically distant but simultaneous VHF outbreaks in European laboratory workers in 1967. The majority of scientific and media attention focused on the most severely affected laboratory, which was in Marburg, West Germany. Infections also occurred in laboratories in Frankfort, West Germany and Belgrade, Yugoslavia.[6,10] All primary cases had either direct contact or contact with tissues derived from African green monkeys imported from a single Ugandan primate exporter.[9] Secondary transmission to both medical personnel and family members was also reported. Thirty-one patients were infected and seven died

(23% mortality). Since 1967, there have been at least 13 additional reports of Marburg virus, most of which manifested as sporadic, isolated, and usually fatal cases in residents and travelers in southeast Africa. However, larger outbreaks such as a 2004-2005 outbreak in Angola that resulted in 200 deaths with a 90% mortality rate have also been reported.[6]

Notably, Ebola and Marburg virus are both reported to persist in immune-privileged tissues of survivors, including the aqueous humor, central nervous system, and testicles. Sexual transmission of both viruses has been reported. In one case, Ebola virus RNA was detected by reverse transcription PCR in semen 531 days following onset of symptoms.[2]

Variants of Marburg virus have been isolated from the Egyptian fruit bat (*Rousettus aegypticus*), which appears to be the natural reservoir, with seasonal circulation changes of Marburg virus in this species being shown to correlate with human infection. Experimentally infected *R. aegypticus* have been found to orally shed Marburg virus despite showing no clinical signs. Marburg virus has also been identified in the urban-dwelling straw-colored bat *(Eidolon helvum)*. In addition to fruit bats, insectivorous bats such as *Miniopterus inflatus* and *Rhinolophus eloquens* have also been implicated.[3]

Interestingly, a third genus of *Filoviridae* was identified in 2011. *Cuevavirus* consists of a single species, *Lloviu cuevavirus,* and was identified following a series of bat die-offs on the Iberian Peninsula. Numerous carcasses of Schreiber's bats (*Miniopterus schreibersii*) and greater mouse-eared bats *(Myotis myotis*) were obtained from the Lloviu Cave in northern Spain, from which the virus is named. All the dead *M. schreibersii* were positive for the virus whereas none was detected in healthy *M. schreibersii* taken from the same location. Although no gross lesions were noted, histopathological signs of viral pneumonia were present.[3]

Participants were unable to definitively identify the cell in the submitted TEM image; however, the vast majority suspected the cell to be a macrophage given the pathogenesis of Marburg virus, in addition to the presence of intracellular cocci and the absence of distinguishing features of other cell lines, such as tight junctions with epithelial cells.

References:

1. Bosio CM, Aman MJ, Grogan C, Hogan R, Ruthel G, Negley D, et al.: Ebola and Marburg viruses replicate in monocyte-derived dendritic cells without inducing the production of cytokines and full maturation. *J Infect Dis* 2003:188(11)**:**1630-1638.
2. Den Boon S, Marston BJ, Nyenswah TG, Jambai A, Barry M, Keita S, et al. Ebola Virus Infection Associated with Transmission from Survivors. Emerg Infect Dis. 2019 Feb;25(2):249-255.
3. Emanuel J, Marzi A, Feldmann H. Filoviruses: Ecology, Molecular Biology, and Evolution. Adv Virus Res. 2018;100:189-221.
4. Geisbert TW, Hensley LE, Gibb TR, Steele KE, Jaax NK, Jahrling PB: Apoptosis Induced In Vitro and In Vivo During Infection by Ebola and Marburg Viruses. *Laboratory Investigation* 2000:80**:**171.
5. Hensley LE, Alves DA, Geisbert JB, Fritz EA, Reed C, Larsen T, et al.: Pathogenesis of Marburg hemorrhagic fever in cynomolgus macaques. *J Infect Dis* 2011:204 Suppl 3**:**S1021-1031.
6. Jahrling PB, Marty AM, Geisbert TW. Viral hemorrhagic fevers. In: Dembek ZF, ed. *Medical Aspects of Biological Warfare*. Washington, DC: Borden

Institute, Walter Reed Army Medical Center, 2007; 271-294.
7. Kuhn JH, Bao Y, Bavari S, Becker S, Bradfute S, Brister JR, et al.: Virus nomenclature below the species level: a standardized nomenclature for natural variants of viruses assigned to the family Filoviridae. *Arch Virol* 2013:158(1)**:**301-311.
8. Martines RB, Ng DL, Greer PW, Rollin PE, Zaki SR: Tissue and cellular tropism, pathology and pathogenesis of Ebola and Marburg viruses. *J Pathol* 2015:235(2)**:**153-174.
9. Miranda MEG, Miranda NLJ: Reston ebolavirus in Humans and Animals in the Philippines: A Review. *The Journal of Infectious Diseases* 2011:204(suppl_3)**:**S757-S760.
10. Ristanović ES, Kokoškov NS, Crozier I, Kuhn JH, Gligić AS. A Forgotten Episode of Marburg Virus Disease: Belgrade, Yugoslavia, 1967. *Microbiol Mol Biol Rev*. 2020;84(2):e00095-19. Published 2020 May 13.
11. van Paassen J, Bauer MP, Arbous MS, Visser LG, Schmidt-Chanasit J, Schilling S, et al.: Acute liver failure, multiorgan failure, cerebral oedema, and activation of proangiogenic and antiangiogenic factors in a case of Marburg haemorrhagic fever. *Lancet Infect Dis* 2012:12(8)**:**635-642.

CASE II: 1235813-015 (JPC 4167863)

Signalment:
Juvenile male intact cynomolgus macaque (*Macaca fascicularis*)

History:
A laboratory primate that was in a control group was dosed intrathecally with radiolabeled imaging medium. Within an hour, the monkey developed vesicular lesions and skin sloughing on the tail, toes, and dorsal aspects of the feet.

Gross Pathology:
The skin of both hind feet was thickened, and there were multifocal abrasions and scabs on the hindfeet and tail.

Laboratory Results:
Haired skin, tail and glabrous skin, footpad: Dermatitis and folliculitis, necrotizing and vesicular, multifocal to coalescing, marked, with keratinocyte apoptosis.

Microscopic Description:
Within the haired skin of the tail and foot, there are multifocal intraepidermal vesicles and bullae characterized by variably sized open spaces within the stratum spinosum filled with loosely organized fibrillar material (fibrin), hemorrhage, small numbers of neutrophils, and few scattered melanin-laden macrophages. These vesicles are occasionally subcorneal, and focally they coalesce resulting in an extensive region of dermal-epidermal separation characterized by the stratum basale separating from the underlying superficial dermis. In a section specially stained with Periodic Acid-Schiff, the highlighted basement membrane is retained along the dermis in this area. The resulting space contains a large amount of fibrin, fluid, macrophages, and neutrophils. Within the separated epidermis and underlying follicular epithelium, keratinocytes of the stratum basale and stratum spinosum are swollen with pale eosinophilic to clear cytoplasm with multifocal large clear vacuoles (ballooning degeneration). Throughout all layers in the epidermis and follicular epithelium, there are multifocal shrunken and hypereosinophilic keratinocytes (apoptosis). Rarely, there are few lymphocytes adjacent to these apoptotic cells. Multifocally, there are small areas of lifted epidermis that have loss of cellular

Figure 2-1. Paw, cynomolgus macaque. There are abrasions and epidermal loss on the digits. (*Photo courtesy of:* Charles River Laboratories – Mattawan, Pathology Department, 54943 North Main St., Mattawan, MI)

detail, hypereosinophilic cytoplasm, and pyknotic nuclei (necrosis). Underlying the lifted epidermis, the superficial dermal collagen is mildly smudged, and superficial small vessels are lined by plump reactive endothelium and surrounded by small numbers of neutrophils and a small amount of hemorrhage and edema. Away from larger bullae and vesicles, the stratum basale and stratum spinosum are mildly to moderately vacuolated (spongiosis). Occasionally, there are free hair shafts within the bullae that are surrounded by moderate numbers of neutrophils and macrophages. There are occasional colonies of bacterial cocci in these areas and within rare follicles.

Contributor's Morphologic Diagnoses: Haired skin, tail and foot: Multifocal to coalescing subepidermal and intraepidermal vesicles and bullae, multifocal keratinocyte apoptosis and necrosis, locally extensive ballooning degeneration and spongiosis, and mild superficial neutrophilic dermatitis.

Contributor's Comment:
Cutaneous adverse drug reactions can occur through several mechanisms and have been reported in macaques.[1,3,6,8,10] First, there could be direct physical or chemical insult to the skin. There could also be indirect toxicity mediated by immune reaction. This occurs with immediate or delayed reactions. The most common cutaneous adverse drug reactions are irritant contact dermatitis and allergic contact dermatitis, which may both be characterized by erythematous macules or vesicles with underlying intercellular edema and superficial dermatitis.[8] Irritant contact dermatitis occurs rapidly after the insult, and acute contact dermatitis is a delayed type IV hypersensitivity reaction. Other possible cutaneous adverse drug reactions include rash with eosinophilia and systemic symptoms (DRESS), generalized exanthematic pustulosis, erythema multiforme (EM), fixed drug eruption, Stevens-Johnson syndrome (SJS) and toxic epidermal necrolysis (TEN).[8] It is important to differentiate these types of lesions from other potential causes of these lesions in macaques such as measles, simian varicella virus, Simian immunodeficiency virus, and pox virus.

In this case, multiple primates presented with similar lesions on the feet and tail after being dosed with a radiolabeled imaging compound. It is important to note that both control and test-article treated animals were affected in this case, and the only common exposure was the radiolabeled substance used for imaging purposes. The monkeys were housed in the same room; however, they were located far apart from each other within the room. There were also other monkeys on the study that had no skin lesions. Animals affected were dosed intrathecally, subcutaneously, or intravenously. Interest-ingly, after switching manufacturers of the isotope, no additional lesions occurred in any other monkeys.

Two monkeys with lesions recovered; however, the others were euthanized for welfare reasons. An inciting cause of these lesions and a precise syndrome were not able to be confirmed; however, this most likely represents an adverse cutaneous reaction to the radiolabeled imaging medium. There was a higher level of the radioactive substance present within the vesicles as compared to the serum of the animals. This accumulation within the vesicles may have exacerbated the lesions. The bacteria present within the lesions are considered to be a complicating factor and not the inciting cause.

Several differential diagnoses were considered in this case based on the clinical presentation, presence of vesicles, bullae, apoptotic cells, and neutrophilic inflammation. Viral etiologies were excluded based on the clinical presentation and absence of characteristic lesions such as inclusions and syncytia.[2,8] Based on the gross and histologic lesions, bullous and necrotizing epidermal diseases were considered as the primary differentials.

The presence of apoptotic cells in all cell layers raised concern for a diagnosis of EM. Characteristically in this disease, there will be single or multiple keratinocytes in a group that are hypereosinophilic, shrunken, and have pyknotic nuclei. These will be present at all levels of the epidermis and extend into hair follicles. Apoptosis is induced by lymphocytes, and these lymphocytes will surround the apoptotic cells (satellitosis).[4,11] The presence of lymphocytes was not a prominent feature observed in this case. There were rarely single lymphocytes in the area of the apoptotic cells. Therefore, while remaining a differential, this condition was considered less likely. In cases of EM there may also be secondary ulceration, crusting, and neutrophilic inflammation. Parakeratosis may also be present in some cases of EM.[4,11]

TEN has been reported to occur with adverse drug reaction, and has been reported in macaques.[1,3] The large areas of apoptosis in this case also histologically resemble toxic epidermal necrolysis; however, the clinical picture does not fit with this condition. In TEN greater than 30% of the skin should be affected, and TEN is a life-threatening condition. In TEN there is also bullous detachment of the epithelium from the dermis, which was observed in some areas in this case. Ultimately this will lead to ulceration. While there may be some lymphocytes present, there are usually present in smaller numbers than in EM. There is also usually little inflammation present.[4,11] It is debated in both the human and veterinary literature whether TEN represents a fulminant form of EM or whether they are distinct disease entities. The clinical picture and progression of disease will aid in distinguishing the two diseases.[11] Additionally, Stevens-Johnson syndrome (SJS) is also considered by some to be related to TEN and EM, and can have similar histologic findings. Due to the clinical picture (less than 30% of skin affected), frequent presence of neutrophilic inflammation, and vesicles within the stratum corneum, TEN was

Figure 2-2. Tail and digital skin, cynomolgus macaque. Large bullae are present within the epidermis of the foot and tail (arrows). (HE, 6X)

considered unlikely, even though there was an area in the tail with detachment of the epidermis from the dermis and presence of apoptotic cells with little inflammation.

Bullous pemphigoid-like disease has also been reported in macaques.[6] This is another disease that can cause blister lesions. In this condition there is development of autoantibody to the bullous pemphigoid antigen, a transmembrane glycoprotein in basal keratinocytes.[4] The dermo-epidermal junction is then separated by proteinases released by granulocytes.[6] The subepidermal separation differentiates this condition from pemphigus vulgaris which may have a similar gross appearance. This condition presents with erythematous macules and vesicles that progress to bullae and ulceration. Typically, both skin and mucous membranes will be affected. Histologically, there will be clean separation between the dermis and epidermis forming a cleft. Neutrophils, eosinophils, and fibrin may be present along the surface of the separated dermis.[4,6] Since some vesicles were intraepidermal, this differential was considered less likely.

Pemphigus vulgaris (PV) is a severe vesiculobullous and ulcerative disease that can occur as a drug reaction.[4] This disease targets the autoantigen desmoglein 3 in the mucous membranes, which is expressed in suprabasilar keratinocytes.[4] Autoantibodies binding to this autoantigen result in acantholytic cells.[4] Cases of PV can present with symmetric transient vesicles, bullae, and ulcers/erosions on the mucous membranes and around areas with friction such as axillary, inguinal, and pressure point areas. Histologically cases will have a suprabasilar cleft. A row of basilar cells will remain along the dermis and will have a rounded "tombstone" appearance.[4] The superficial dermis may be infiltrated by variable numbers of lymphocytes, plasma cells, and neutrophils. In some areas in the present case, there was a single remaining layer of basilar keratinocytes; however, these cells did not have the classic tombstone appearance, and this was not a consistent feature. There were some rounded keratinocytes around vesicles; however, these were interpreted as apoptotic rather than acantholytic cells. Thus, pemphigus vulgaris was also considered unlikely.

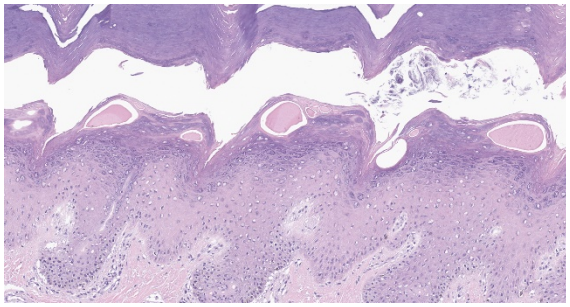

Figure 2-3. Digital skin, cynomolgus macaque. Vesicles arise within the granular cell layer. (HE, 130X)

One possible etiology for the lesions observed in this monkey was irritant contact dermatitis. It was speculated that perhaps the isotope may have been passed in urine, and the affected areas (feet and tail) would be the most likely to come into contact with the irritant. The initial gross lesions in irritant contact dermatitis are erythema and papules followed by exudation, scaling and crusting.[4] With chronic exposure, lichenification, hyperpigmentation, and alopecia can develop.[4] The affected sites usually have sparse hair or are hairless due to the protective aspect of the hair-coat. Pruritus can occur but its presence is variable.[4] Histologically, the condition is characterized by epidermal necrosis with subepidermal separation and neutrophilic dermatitis. Early in the course of the disease, there may just be epidermal spongiosis and small vesicles. In chronic lesions, there may be parakeratosis, acanthosis, and serous and neutrophilic crusts. There may be variable superficial

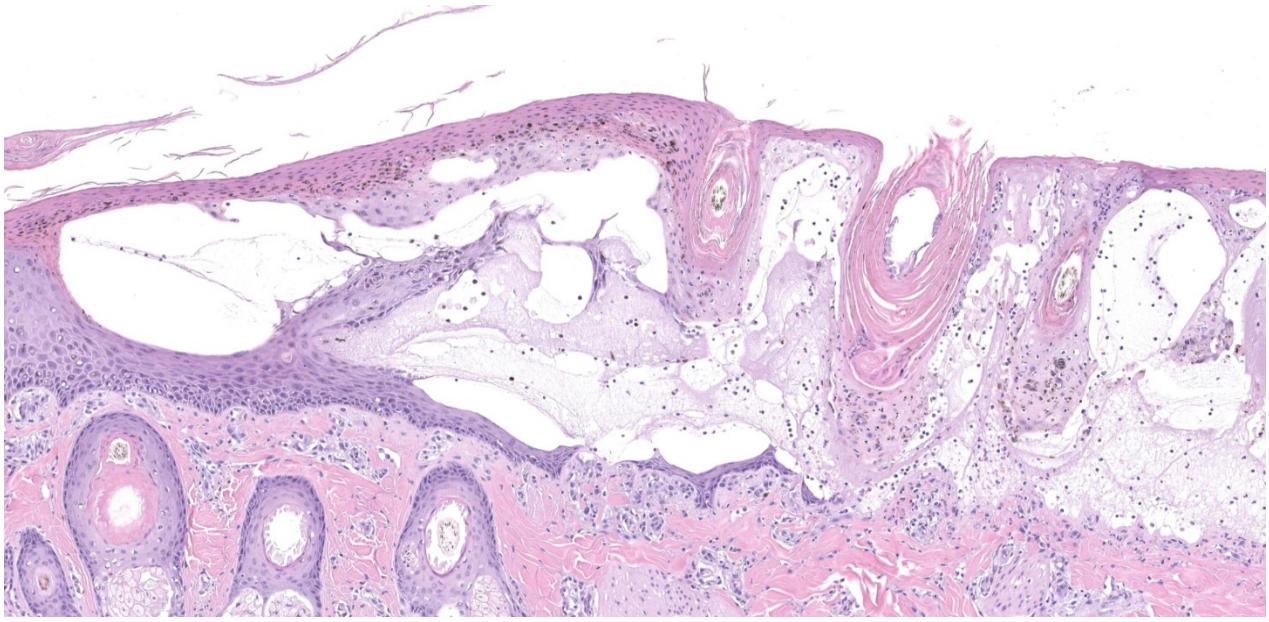

Figure 2-4. Tail skin, cynomolgus macaque. Vesicles arise within the granular cell layer (left) and as they coalesce, the full epidermis is lifted off the underlying dermis. Vesicles contain abundant proteinaceous fluid, fibrin, and infiltrating neutrophils. The roof of the vesicles is composed of necrotic epithelium, which incorporates hair follicles. (HE, 86X)

perivascular mixed inflammation.[4] Based on the intraepidermal vesicles, neutrophilic inflammation, irritant contact dermatitis was considered; however, again this does not entirely explain the clinical history and presentation. Ultimately, the disease process in this case is considered a cutaneous drug reaction to the radiolabeled imaging medium. While the histologic features do not entirely fit with the discussed differentials, the presence of vesicular and bullous lesions in combination with the clinical history support this conclusion.

Contributing Institution:
Charles River Laboratories, Mattawan, MI

JPC Diagnosis:
Oral mucosa and haired skin: Epithelial necrosis, coagulative, focally extensive, with subepithelial clefting, ulceration, nuclear streaming of the stratum basale, and subepithelial collagen homogenization and edema.

JPC Comment:
The contributor provides a truly outstanding review of the clinical and histologic features of various forms of cutaneous drug reactions in addition their pathogeneses.

The moderator discussed the importance and value of detailed written descriptions, particularly in regard to the research setting, with this case being a prime example. Given the histologic lesions do not completely meet the criteria of the differentials, the histologic description itself is a useful tool for investigators. In addition, thorough descriptions of what are believed to be already known conditions at the time of writing may in turn retrospectively facilitate the discovery of new entities.

Although unlikely in this case, especially given these cynomolgus macaques were housed indoors, an additional consideration in regard to the development of dermatitis in animals receiving a xenobiotic is cutaneous phototoxicity (i.e. photosensitivity). Cutaneous photosensitivity is a nonimmunologic form of dermatitis induced by cutaneous photoactive agents in the presence of ultraviolet radiation (predominately type A (UVA) light).[9] Photosensitivity is a dose-dependent phenomenon with respect to both

the photoactive compound and light exposure.[5]

When exposed to ultraviolet radiation, phototoxic compounds form stable photoproducts that directly cause cell damage or enter an excited state, forming both free radicals and reactive oxygen species that cause direct cell damage and oxidize cellular lipids (e.g. membranes), respectively.[5]

There are three types of photosensitivity (types I-III), which are classified in regard to the source of the photoactive agent.[7]

Type I photosensitivity (also known primary photosensitization) predominately occurs as the result of photoactive compounds being ingested, absorbed, and deposited in the skin, although phytophotocontact dermatitis as the result of direct adsorption of compounds into the skin has also been reported. Herbivores are commonly affected as plants are the most common source of ingested photoactive compounds. St. John's wort (*Hypericum performatum),* buckwheat (*Fagopyrum* spp.), spring parsley (*Cymopterus watsonii*) and bishops weed (*Ammi majus*) are a few examples of plants containing photoactive pigments.[7]

Type I photosensitivity may also occur following the administration of medications with photoactive properties. In general, these medications typically have a low molecular weight (200-500 Daltons) and have planar, tricyclic, or polycyclic configurations. However, no elements or configurations automatically impart phototoxicity to compounds. Phototoxic medications include numerous commonly used prescription and over the counter products; one recent report identified 393 medications with evidence of photosensitization, although many medications were historical and are no longer in use today. Medications with high evidence of photosensitization (i.e. ≥15 publications) include (but are not limited to) hydrochlorothiazide, furosemide, amioda-rone, naproxen, ketoprofen, piroxicam, lemefloxacin, ciprofloxacin, tetracycline, doxycylcine, griseofulvin, quinine, and promethazine.[5]

An additional concern in regard to photosensitizing medications is the potential for photocarcinogenic effects, particularly in regard to the development of skin cancer (e.g. squamous cell carcinoma (SCC), basal cell carcinoma (BCC), and melanoma) in humans. Photocarcinogenesis is the subject of controversial scientific discussions and debate as probable mechanisms remain under investigation. The relationship between photosensitive medications and photocarcinogenesis is likely based on multiple factors, including patient age, susceptibility to solar radiation, cumulative dose of medications, and other unknown factors. Psoralens (furocomarins) are associated with the strongest evidence for photocarcinogenic effects; these substances have been investigated in animal and human models, with studies demonstrating increased risk of SCC, BCC, and melanoma. However, multiple medications have been reported to be associated with an increased risk of skin cancer in humans, including NSAIDs and fluroquinolones, thiazide diuretics, tetracyclines, amiodarone, and voriconazole amongst others.[5]

Type II photosensitivity occurs as the result congenital enzyme deficiencies that result in the accumulation of photodynamic endogenous pigment in the skin due to abnormal heme-synthesis. Deficiency of uroporphyrinogen III cosynthase is a classic example in bovines that results in the deposition and accumulation of porphyrin pigments in many tissues, including the bone and teeth, as well as the skin. Uroporphyrins

in the skin are particularly reactive to UVA radiation. Following activation, these pigments cause the formation of membrane damaging reactive oxygen species either directly and/or potentially via activation of the xanthine oxidase pathway.[7]

Type III photosensitivity is the most common form of photosensitivity in domestic animals and occurs as the result of impaired hepatic clearance of phylloerythrin as the result of either hepatocellular damage or biliary obstruction. Phylloerythrin is a photoactive substance derived from chlorophyll that is normally formed within the digestive tract, absorbed, transported to the liver via portal circulation, and then excreted in the bile. Hepatotoxic plants such as lanata (*Lantana camara*) or mycotoxins such as sporidesmin, inhibit the hepatic clearance of phylloerythrin, resulting in its accumulation in the skin and subsequent development of cutaneous lesions.[7]

Histologic lesions associated with cutaneous photosensitization include coagulative necrosis of the epidermis with variable extension to adnexal structures and the superficial dermis, subepidermal clefts, dermal edema, and swollen or necrotic blood vessels that may demonstrate fibrinoid degeneration with variably present thrombosis. There is typically scant inflammation early in the process; however, the tissue is soon infiltrated by neutrophils.[7]

References:

1. Allen KP, Funk AJ, Mandrell TD. Toxic epidermal necrolysis in two rhesus macaques (*Macaca mulatta*) after administration of Rituximab. *Comp Med*. 2005;55(4):377-381.
2. Bernstein JA, DIdiert PJ. Nonhuman primate dermatology: a literature review. *Vet Dermatol.* 2009;20(3):145-156.
3. Garman RH, Reed C, Blick DW. Toxic epidermal necrolysis in a monkey (*Macaca fascicularis*). *Vet Pathol.* 1979;16:81-88.
4. Gross TL, Ihrke PJ, Walder EJ, Affolter VK. *Skin Diseases of the Dog and Cat: Clinical and Histopathologic Diagnosis.* 2nd ed. Blackwell Science Ltd; 2005.
5. Hofmann GA, Weber B. Drug-induced photosensitivity: culprit drugs, potential mechanisms and clinical consequences. *J Dtsch Dermatol Ges*. 2021;19(1):19-29.
6. Kim JM, Kim HJ, Min BH, et al. Bullous pemphigoid-like skin blistering disease in a rhesus macaque. *J Med Primatol*. 2016;45:206-209.
7. Mauldin EA, Peters-Kennedy J. Integumentary system. In: Maxie MG, ed. *Jubb, Kennedy, and Palmer's Pathology of Domestic Animals*. Vol 1. 6th ed. Louis, MO: Elsevier; 2016:577-580.
8. Mecklenburg L, Romeike A. Recommended diagnostic approach to documenting and reporting skin findings of nonhuman primates from regulatory toxicity studies. *Tox Pathol*. 2016;44(4):591-600.
9. Ngo MA, Maibach HI. Dermatotoxicology: historical perspective and advances. *Toxicol Appl Pharmacol*. 2010;243(2):225-238.
10. Palanisamy GS, Marcek JM, Cappon GD, et al. Drug-induced skin lesions in cynomolgus macaques treated with metabotropic glutamate receptor 5 (mGluR5) engative allosteric modulators. *Tox Pathol*. 2015;43:995-1003.
11. Yage JA. Erythema multiforme, Stevens-Johnson syndrome and toxic epidermal necrolysis: a comparative review. *Vet Dermatol*. 2014;25:406-e64.

CASE III: 18-33 (JPC 4135937)

Signalment:
8-week-old female ragdoll kitten (*Felis catus*)

History:
The kitten was shut in a closet overnight, and in the morning was found by the owner curled up on the floor in the closet with red-brown, gelatinous material oozing from her mouth. The owner identified a live wire protruding from the floor that shocked her when touched. The kitten was subsequently presented to an emergency veterinarian for further evaluation. On physical examination, the cat was markedly painful around the mouth, dull, and weak. Numerous extensive burn wounds were identified on the lips, tongue, and palate. Given the extent of the lesions and poor prognosis for healing of wounds in the oral cavity, the kitten was euthanized.

Gross Pathology:
There was moderate, regional swelling within the soft tissues surrounding the mandible and ventral neck. Multifocally at the oral commissures, along the mandibular and maxillary gingiva, on the rostral 1/3 of the tongue, and the rostral half of the hard palate to the level of the maxillary incisors, were variably sized (2 – 20 mm diameter) full thickness ulcerations covered by brown to gray to black, friable and sloughing tissue. Multifocally, tissue surrounding ulcers was discolored pale tan to gray. Additionally, on internal examination there was regional dark red discoloration of caudodorsal lung fields.

Laboratory Results:
Upon admission to the veterinary hospital, a complete blood count (CBC) and serum biochemistry panel were performed. CBC revealed a mild neutrophilia (interpreted as a stress leukogram) and moderate

Figure 3-1. Oral cavity, cat. There is multifocal to coalescing ulceration, necrosis, and brown to black discoloration of the tongue, lips, and hard palate, consistent with electrothermal injury. (*Photo courtesy of:* North Carolina State University, College of Veterinary Medicine, Department of Population Health and Pathobiology. https://cvm.ncsu.edu/research/departments/dphp/programs/pathology)

thrombocytosis. Significant serum biochemistry panel findings included a markedly elevated creatinine kinase (10,397 IU/L; RR 60 – 531 IU/L), mildly elevated AST (166 IU/L; RR 11 – 40 IU/L), and a mild hyperkalemia (5.7 mmol/L; RR 3.5-5.1 mmol/L). All of these findings were considered attributable to regional skeletal muscle damage from electrothermal injury.

Microscopic Description:
Tongue and Lips: Four sections of tongue and three sections of lip skin are examined and have similar histologic features that are described together. Multifocally, there is variable intraepidermal/mucosal and/or subepidermal/mucosal clefting, resulting in multifocal vesicle formation, erosion, and regionally extensive detachment of the epithelium/mucosa (ulceration). There is multifocal to coalescing nuclear elongation/streaming of basal cells in a "fish bone" type pattern, and affected nuclei are hyperchromatic to pyknotic. At the areas of ulceration and vesicle formation, there are multifocal aggregates of mixed bacterial organisms (rods and cocci), mild multifocal hemorrhage, and occasional aggregates of

black granular material (presumptive metallization). In the rostral third to half of examined sections of tongue, and variably identified in examined skin sections, there is loss of distinction of dermal/submucosal collagen fibers, which gradually merge into an amphophilic, amorphous coagulum (collagen homogenization). When viewed with polarized light, this collagen lacks normal birefringence. Multifocally within the dermis and submucosa, the walls of vessels are smudged with nuclear pyknosis and streaming. Multifocally, skeletal muscle fibers exhibit sarcoplasmic hypereosinophilia and vacuolation, loss of cross striations, and nuclear pyknosis. In some sections, there is mild to moderate, multifocal edema with scattered intermixed hemorrhage within the submucosa and between individual myofibers.

Perl's Prussian blue and rhodanine histochemical stains are applied to tissues. Multifocally, black granular material and adjacent necrotic tissue exhibits strong positive staining for copper

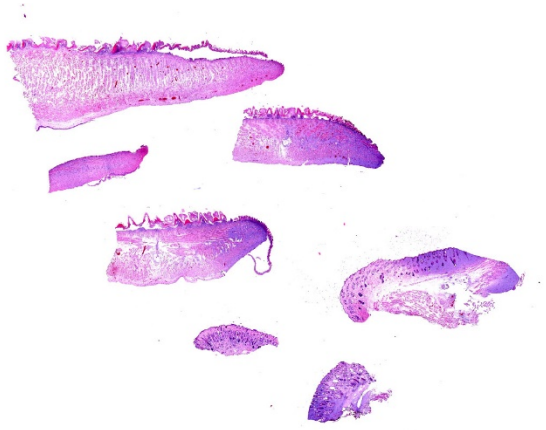

Figure 3-2. Tongue and haired skin, cat. Four sections of tongue (top and left) and three of the haired skin of the lip (bottom and right) are submitted for examination. At subgross magnification of the tongue, there is peripheral loss of the mucosal epithelium and liftin of epithelium at the edge of the lesion. There is focally extensive bluish discoloration of soft tissues in both the tongue and skin. (HE, 6X)

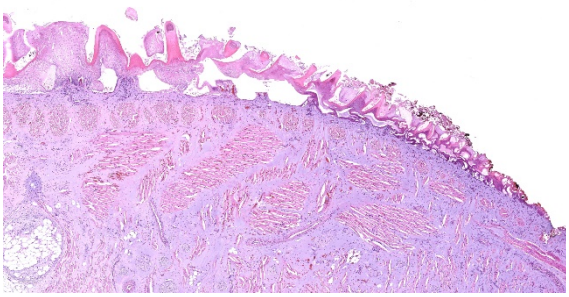

Figure 3-3. Tongue, cat. The mucosal epithelium is diffusely necrotic and lifted off of the lamina propria by coalescing subepithelial vesicles. At the edge of the lesion, mucosal epithelium is reduced to a coagulum with a dark black discoloration. Throughout the section, submucosal and interstitial collagen is homogenized and amphophilic. There is loss of epithelium on the underside of the tongue as well. (HE, 36X)

Contributor's Morphologic Diagnoses: Lips and tongue: Marked, regionally extensive, coagulative necrosis with subepidermal and intraepidermal clefting, multifocal ulceration, epidermal nuclear streaming, collagen homogenization, and metallization (consistent with electrothermal injury)

Contributor's Comment:
This is a case of clinically confirmed electrocution for which multiple classic histologic features are present.

In veterinary patients, electrical injuries most commonly occur as accidents or, in the case of outdoor grazing animals, lightning strike.[4] Accidental electrical injuries can be further delineated into either low or high voltage exposure. In this case, accidental electrocution occurred from chewing on a live electrical wire connected to a household circuit, which is most consistent with a low voltage exposure. In general, high voltage exposure should theoretically have a higher propensity for more extensive injury. However, as seen in this case, low voltage accidents can result in profound external injury (electrothermal burn) with prolonged contact [4], a small contact surface area, and

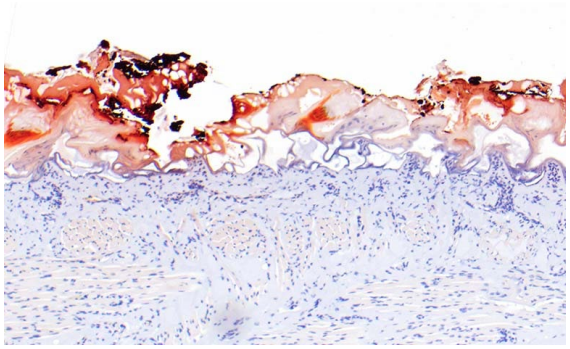

Figure 3-4. Tongue, cat. Black granular material present amongst necrotic epithelium as well as the necrotic epithelium itself exhibits multifocal positive staining for copper (consistent with metallization). (Rhodanine, 400X) *Photo courtesy of:* North Carolina State University, College of Veterinary Medicine, Department of Population Health and Pathobiology. https://cvm.ncsu.edu/research/departments/dphp/programs/pathology)

with a media (saliva) to further promote electrical conduction.

Characteristic microscopic features of electrothermal burns resulting from electrocution include changes to both the epidermis and dermal collagen as well as deposition of metal within affected tissue, all of which are present in this case.

First, within the epidermis, there is formation of both intra- and subepidermal vesicles, which form a "honeycomb pattern" when numerous vesicles are present adjacent to one another.[4] Furthermore, there is profound elongation of epidermal cells, with tight packing of pyknotic, elongated nuclei, also termed a "fishbone-like" elongation.[4] This feature was previously thought to be due to polarization of cells from the passing of electrical current, but has since been instead postulated to be secondary to heat injury, as the same morphologic feature can be seen in flame injury burns.[2]

Second, within the dermis, collagen fibers lose distinction and instead can form a large coagulum, known as "collagen homogenyization.[2,3]" Affected collagen stains basophilic, and has loss of birefringence when viewed under polarized light. Depending on the extent of injury, this homogenization can extend and affect collagenous stroma in various deeper tissues, such as those surrounding vessels and nerves in this case.

Third, microscopic beads of metal can be transferred from conductive metals to the affected tissue, a phenomenon known as "metallization.[4]" This finding is not specific for electrocution, as it can also be seen in thermal injury from fires. However, metalization in cases of electrocution has been noted more likely to be concentrated at the margins of wounds, or penetrate deeper into tissues. In contrast, in cases of flame injury metal tends to be more diffusely but superficially distributed.[4] Histochemical stains for iron and copper can aid in identification of metal within tissues. In this case, black granular pigment was present in the epidermis of the tongue along margins of necrosis and in severely affected areas. Perl's Prussian blue and rhodanine histochemical stains were applied to tissues, and granular material exhibited strong positive staining with rhodanine stain, confirming the presence of copper metallization. Additional small positive staining beads were also present throughout the necrotic epithelium.

From a forensic perspective, when investigating the nature of external lesions in which electrocution is suspected, it can be challenging to both grossly and histologically differentiate lesions caused by electrocution, flame, or impact (abrasions).[2] While the previously described microscopic features are most commonly seen in cases of electrocution, these features can also variably be seen in either flame injury or impact abrasions.[2] In a study comparing histologic changes from these injuries in humans, tight packing of pyknotic nuclei was the most

specific feature distinguishing electrocution injury from flame injury or impact abrasions.[2] Given the overlap in histologic features that can be seen in these injuries, extensive investigation into clinical history, if possible, is helpful in case work up. In this case, the clinical history of this patient confirms that identified lesions can be attributed to electrocution.

In addition to tissues on the submitted slide, similar lesions were also present on examined sections of hard palate and adjacent nasal turbinates, with rare evidence of Wallerian-type degeneration in peripheral nerve fibers captured in section.

In addition to external injuries incurred from electrical injury, internal injuries are also possible, and organs affected depend on the flow of current through the body, with endothelial cells, muscle (skeletal and cardiac), and central nervous system most often being affected. Internal injury is rare in cases of low-voltage electrocution, and in this case, there was no evidence either clinically or on postmortem examination of injury to the heart or central nervous system. However, this patient did have gross and histologic evidence of non-cardiogenic (caudodorsally distributed) pulmonary edema, which can be seen in cases of low voltage electrical injury.[5,6] The patho-physiology of electrocution-induced pulmonary edema is not completely understood, but is thought to be caused by either direct endothelial damage from electricity, or represent a form of neurogenic pulmonary edema, in which catecholamine release results in pulmonary hypertension and increased vascular permeability.[1]

Contributing Institution:
North Carolina State University, College of Veterinary Medicine, Department of Population Health and Pathobiology
https://cvm.ncsu.edu/research/departments/dphp/programs/pathology

JPC Diagnosis:
Oral mucosa and haired skin: Epithelial necrosis, coagulative, focally extensive, with subepithelial clefting, ulceration, nuclear streaming of the stratum basale, and subepithelial collagen homogenization and edema.

JPC Comment:
The contributor provides an excellent review of histologic lesions associated with electrothermal injury, a potentially challenging diagnosis to determine in cases lacking sufficient history and context.

There are multiple classifications in regard the voltages associated with the power grid, including high, moderate, and low. High voltage transmission lines are typically equal to or greater than 60 kilovolts (kV). Moderate voltages are typically associated with local distribution lines, which carry electricity from distribution stations to residences and businesses; their voltage typically ranges from 2.4-60kV. Transformers lower the distribution line voltage to 600V or less (i.e. low voltage) prior to the current entering individual service lines connected to homes. For simplification, some publications discussing electrocution associate the term "low-

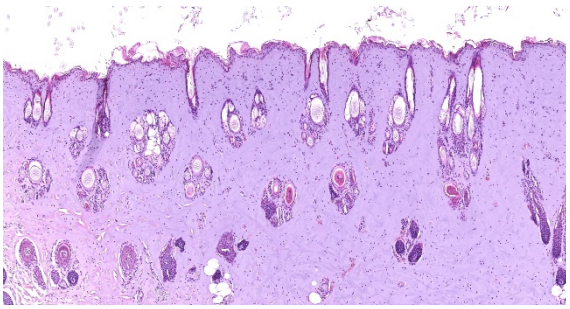

Figure 3-5. Haired skin, lip, cat. There is diffuse necrosis of mucosal epithelium follicles and adnexa extending into the deep dermis. There is diffuse homogenization of collagen and individual collagen fibers can no longer be determined. (HE, 73X)

voltage" with less than 600V whereas those with greater than 600V are “high voltage”.[3]

Electrocution occurs when an animal makes contact with two pieces of electrical equipment (e.g. power lines) or is in contact with both electricity and a grounded object. Once the circuit is established, the electricity’s path determines which tissues are affected, which are typically those occupying the shortest distance between the entry and exit points in high-voltage situations. The most likely cause of death in high-voltage situations is the result of current passing through the cardiac and/or respiratory centers of the CNS or directly through the heart, resulting in cardiac and/or pulmonary arrest. Notably, ventricular fibrillation precedes cardiac arrest in low voltage electrocutions but does not occur in high voltage electrocutions.[3]

Two forms of electrothermal injury occur at the cellular level, with the type of injury dependent on the cell’s size as well as its resistance to electrical current. The passage of electrical current through tissues generates heat, which in turn results in the formation of pores in cell membranes in a process known as electroporation. Electroporation typically affects larger cells, such as neurons and myocytes, while also correlating with the current’s path. In contrast, thermal injury is more likely to occur in regions of higher resistance, such as the epidermis and dermis in this case.[3]

Electrocution is a significant problem in large birds, such as raptors. A review evaluating necropsy methods and findings associated with power line electrocution in raptors found 18% had a single external burn measuring less than 3cm. In cases where electrocution injury is not clear, the author recommends close evaluation of the undersides of wings distal to the elbow and

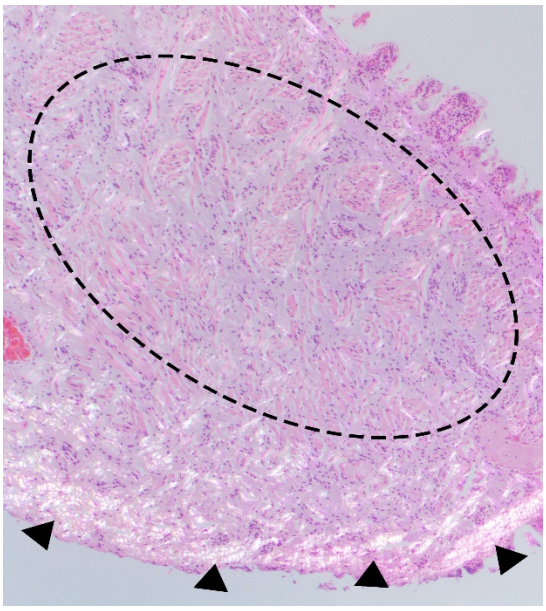

Figure 3-6. Tongue, cat. Homogenized collagen within the tongue has lost birefringence. (HE with polarized light, 40X). *Photo courtesy of:* North Carolina State University, College of Veterinary Medicine, Department of Population Health and Pathobiology. https://cvm.ncsu.edu/research/departments/dphp/programs/pathology)

lower legs and feet, which were the most common location for small isolated burns. In addition, charred tissues (e.g. skin, feathers, and beak keratin) exposed to an alternate light source at 530-570 nm under a red filter will photoluminesce bright red; unaffected or dirty tissues will photoluminesce poorly or not at all. Electrocution should always be considered as a differential for dead birds found under power lines; however, a thorough necropsy is required for this diagnosis as other possible causes of death in these areas include collisions and gunshot. The majority of avian electrocutions are reported to occur in association with distribution lines.[3]

A historical review of the early study of the pathophysiology associated with electrocution, as well as electricity’s paradoxical ability to save lives, provides for an interesting detour.

Commercially available electricity became increasingly popular following the invention practical generators during the 1870s, which was inherently associated with many accidental deaths, particularly amongst utility workers. Early hypotheses in regard to the pathogenesis of electrocution included theories such as arterial blood's loss of magnetic properties. Medical interest was so great at the time that 12 physicians attended the execution of William Kemmler, the first legal execution by electrocution, on August 6th 1890. Although an extensive autopsy was performed, the underlying cause of death remained largely unknown.[1]

In 1899, Italian physiologists Jean Louis Prevost and Frederic Battelli as well as Columbia University's RH Cunningham independently demonstrated strong electrical current stopped the hearts of experimental animals while weaker shocks caused ventricular fibrillation, also resulting in death. In addition, Prevost and Battelli noted some cases demonstrating ventricular fibrillation were restored to a normal sinus rhythm after a second shock was applied to electrodes in the mouth and the intestine, unknowingly performing the first successful internal defibrillation. The significance of the event went largely unnoticed at the time since ventricular fibrillation was thought to only occur in animals and the phenomenon could not be consistently replicated nor explained.[1]

The invention of the electrocardiograph greatly facilitated the understanding of cardiac electrophysiology, with the first account of a recorded electrocardiograph attributed to Augustus Desire Waller in 1887. It was developed into a clinical tool over the following decades, greatly enhancing the understanding of arrhythmias and cardiac physiology. Notably, researchers identified a refractory period in the cardiac cycle during which the ventricles were more susceptible to ventricular fibrillation as the result of an electrical shock. Carl Wiggers and Rene Wegria conclusively demonstrated this in 1940, finding that a brief electrical shock only 'induces fibrillation when the shocks fall during the vulnerable period of late systole'.[1]

The first successful human defibrillation was performed by Claude Beck in 1947 on a 14-year old boy suffering ventricular fibrillation during an operation for pectus excavatum during which the thorax was already open. The paddles were applied directly to the heart and four shocks of 110V were delivered, saving the boy's life.[1]

References:

1. Ball CM, Featherstone PJ. Early history of defibrillation. *Anaesth Intensive Care*. 2019;47(2):112-115.
2. Caswell JL and Williams KJ. Respiratory System. In: Maxie MG, ed. *Jubb, Kennedy, and Palmer's Pathology of Domestic Animals.* Vol 2. 6th Ed. St. Louis, Elsevier; 2016: 487-489.
3. Kagan RA. Electrocution of Raptors on Power Lines: A Review of Necropsy Methods and Findings. *Vet Pathol*. 2016;53(5):1030-1036.
4. Sangita C, Garima G, Jayanthi Y, Arneet A, Neelkamal K. Histological indicators of cutaneous lesions caused by electrocution, flame burn and impact abrasion. *Med Sci Law*. 2018;58(4):216-221.
5. Schulze C, Peters M, Baumgärtner W, Wohlsein P. Electrical Injuries in Animals: Causes, Pathogenesis, and Morphological Findings. *Vet Pathol*. 2016;53(5):1018-1029.
6. Singh S, Sankar J, Dubey N. Non-cardiogenic pulmonary oedema following accidental electrocution in a toddler. *BMJ Case Rep*.

2011;2011:bcr0120113749. Published 2011 Apr
7. Truong T, Le TV, Smith DL, Kantrow SP, Tran VN. Low-voltage electricity-induced lung injury. *Respirol Case Rep*. 2017;6(2):e00292. Published 2017 Dec 22.

CASE IV: 18042E (JPC 4136503)

Signalment:
Four-year-old, male rhesus macaque (*Macaca mulatta*)

History:
This animal was exposed to 10.7 Gy whole thorax irradiation using 6 MV linear accelerator-derived photons delivered at a dose rate of 100 cGy/min using methods similar to those previously described.[2] The animal was euthanized 63 days post-irradiation due to an elevated respiratory rate (experimental endpoint).

Gross Pathology:
The lungs were more than twice the normal weight with patchy mottled red/brown regions in all lobes (consolidation).

Laboratory Results:
None submitted.

Microscopic Description:
About 80% of alveolar lumina contain eosinophilic homogeneous material (edema), forming hyaline membranes in some, and foamy macrophages and eosinophils. Alveolar spaces are intermittently expanded 2-8 times normal by clear space (emphysema) and adjacent alveoli are collapsed (atelectasis). Alveolar septa are thickened 4-5 times normal by fibrillar eosinophilic material (collagen), eosinophils, plasma cells, and macrophages. Type II pneumocytes are prominent, and many are binucleated with karyomegaly and loss of polarity.

Contributor's Morphologic Diagnoses:
Lung: Pneumonitis, diffuse, chronic, severe with alveolar histiocytosis, type II pneumocyte hyperplasia and dysplasia, and interstitial fibrosis.

Contributor's Comment:
Findings in this case are consistent with exposure to ionizing radiation. Radiation-induced lung injury has been divided into two syndromes.[3,6] The first is radiation-induced pneumonitis which occurs within months of exposure and is further subdivided into phases. The latent phase lacks histologic damage and is clinically silent. Ultrastructural studies, however, have revealed increased capillary permeability, degenerate mitochondria, and abnormal lamellar bodies in type II pneumocytes. The exudative phase is characterized by excessive

Figure 4-1. Lungs, rhesus macaque. The lungs were more than twice the normal weight with patchy mottled red/brown regions in all lobes. (*Photo courtesy of*: Section on Comparative Medicine, Wake Forest School of Medicine, Medical Center Boulevard, Winston-Salem, NC 27157, http://www.wakehealth.edu/Comparative-Medicine/)

leakage of fibrin into alveolar spaces which contributes to the formation of hyaline membranes. During this acute pneumonitis, alveoli are hypercellular primarily due to foamy macrophages. The second syndrome is the late stage of radiation-induced lung injury and is characterized by pulmonary fibrosis. This phase is associated with abundant collagen fibers in the interstitium. Radiation-induced fibrosis then results in progressive dyspnea due to decreased lung compliance and impaired gas exchange.

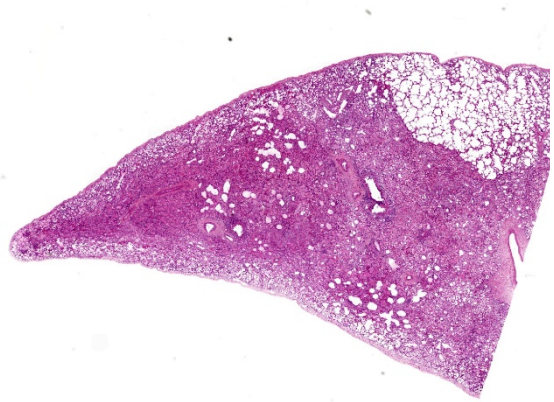

Figure 4-2. Lung, rhesus macaque. At subgross magnification, 80% of the lung is consolidated and the remaining (top right) demonstrates mild emphysema. (HE, 5X)

The extent to which cells are damaged by radiation is based on both physical and biological factors.[3] Physical factors include the dose of radiation, usually expressed in Gray, and the period of time over which the radiation is delivered (single, fractionated, or protracted). Biological factors include features of the cell type exposed and how often it divides. Rapidly proliferating cells are more sensitive to injury with irradiation, and differentiated cells are less sensitive. For example, proliferating hematopoietic stem cells in the bone marrow are relatively sensitive while differentiated nervous system cells are resistant. For single dose whole-chest exposures in humans, the dose-response curve is steep, with a 50% incidence of pneumonitis at around 10 Gy.[10] The dose-response relationship is similar for macaques.[2,8] Concurrent cardiac effects may contribute to pulmonary edema or pleural effusion.

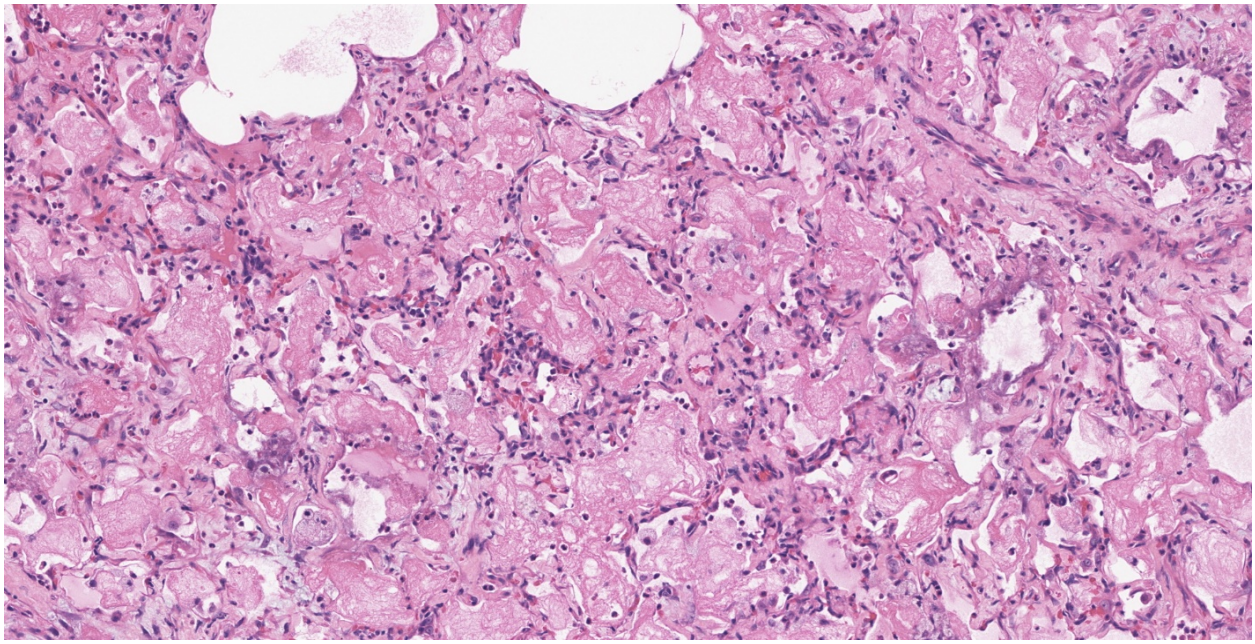

Figure 4-3. Lung, rhesus macaque. Within the areas of consolidation, alveoli are filled with various combinations of edema, fibrin, macrophages, and neutrophils. Septa are markedly expanded by edema, fibrin, and variable infiltrate of neutrophils and macrophages. (HE, 171X)

As ionizing radiation passes through tissue, it interacts with intracellular water to generate highly reactive free radical species. Anti-oxidants or detoxifying enzymes are then upregulated to enhance cellular defense mechanisms in response. The overexpression of manganese superoxide dismutase during the late fibrotic response in a mouse model of radiation-induced pneumonitis is one example.[5] If injury persists, irradiation disrupts the cellular redox balance because of the production of abundant reactive oxygen species. This leads to oxidative damage to DNA, protein, and lipid peroxidation which incites an inflammatory response.[9] Despite extensive research, target cells or clear mechanisms underlying radiation-induced lung injury are not fully understood. Among the inflammatory cells, macrophage polarization is considered as an important axis for the control of fibrosis. Radiation-induced injury activates M1 macrophages leading to the initial stage of radiation-induced pneumonitis, and the M2 phenotype has been linked with radiation-induced fibrosis.[4] Among pro-fibrotic cytokines, TGF beta plays a major role in fibrogenesis, particularly in the transformation of fibroblasts to myofibroblasts, which is an important stimulus for the production of extracellular matrix.[8]

Contributing Institution:
http://www.wakehealth.edu/Comparative-Medicine/

JPC Diagnosis:
Lung: Pneumonia, interstitial, fibrino-necrotic and eosinophilic, diffuse, severe, with hyaline membranes, interstitial fibrosis, and type 2 pneumocyte hyperplasia.

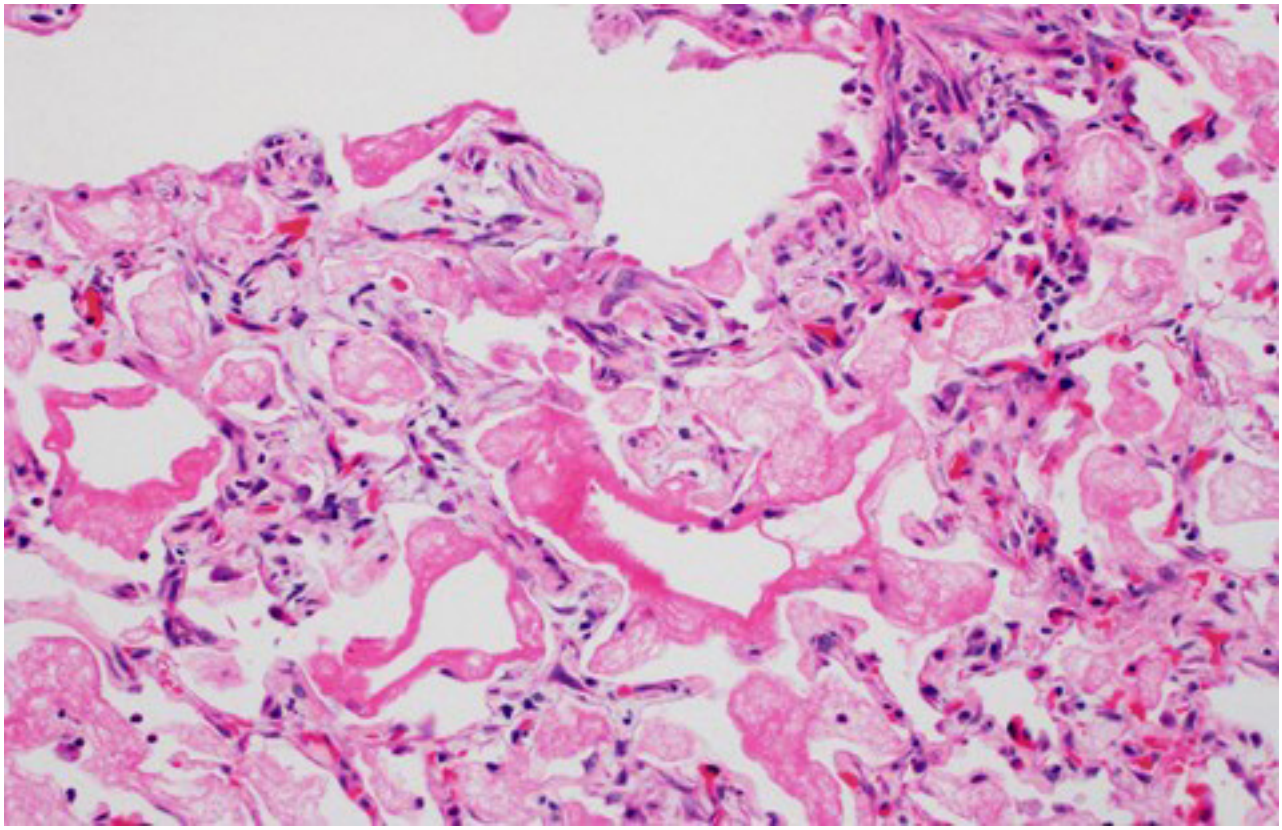

Figure 4-4. Lung, rhesus macaque. There is flooding of alveoli with fibrin, which occasionally compacts to form hyaline membranes lining damaged alveolar septa. (HE, 378X)

JPC Comment:

Radiotherapy (RT) is a common and effective component of multiple oncologic treatment protocols and has been associated with decreases in local recurrence, distant metastases, and mortality of certain cancers. However, radiation induced lung injury is an inherent risk of RT, particularly in breast and lung cancer patients as lung tissue will invariably be exposed to the radiation portal.[7] Approximately 43% of lung cancer patients receiving a total dose of 27.5Gy or more will develop radiation induced lung injury[1] and up to 16% of breast cancer patients are affected by radiation pneumonitis and subsequent fibrosis.[7] These patients are affected by the two consecutive syndromes described by the contributor, with radiation pneumonitis occurring <6 months following RT followed by radiation induced pulmonary fibrosis.[7]

As noted by the contributor, the development of radiation-induced lung injury is influenced by factors such as the radiation dose as well as the timespan of exposure. Since individual cases vary, oncologists must carefully select optimal protocols based on individual patient factors. For example, common breast cancer protocols utilize either hypofractionated (42.56Gy in 16 fractions) or conventionally fractionated (50Gy in 25 fractions) protocols over several weeks. Corticosteroids are commonly used a primary treatment of radiation induced pneumonitis, followed by a tapering schedule.[7]

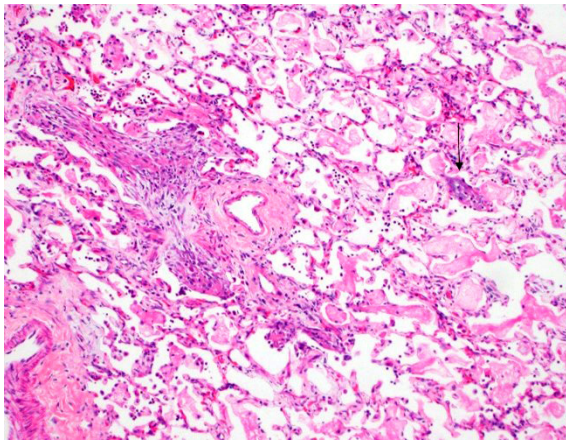

Figure 4-5. Lung, rhesus macaque. At left, an airway lumen is filled with proliferating fibroblasts and collagen (bronchiolitis obliterans). At right, airway, there is a focus of septal necrosis with dystrophic mineralization. (HE, 100X)

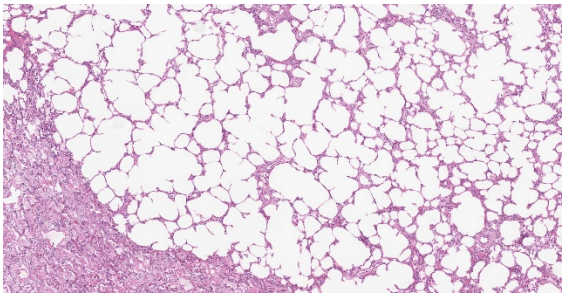

Figure 4-6. Lung, rhesus macaque. There is mild emphysema of the adjacent less affected lung. (HE, 52X)

Clinically, radiation pneumonitis in human patients is a diagnosis of exclusion after differentials such as disease progression, tuberculosis, and asthma are ruled out, followed by chest radiographs, computed tomography scans, and/or pulmonary function tests. However, antemortem diagnosis of radiation pneumonitis is difficult as there are no definitive radiological or laboratory tests.[7]

Radiation-induced lung injury investigations have commonly utilized murine models, particularly the C57BL/6J strain. Similar to NHPs and humans, the threshold single dose required to elicit pathogenesis also appears to be 10Gy. C57BL/6J mice typically develop radiation pneumonitis 8-16wks following exposure, followed by pulmonary fibrosis starting at 24 weeks. Interestingly, C3H and CBA strains develop radiation pneumonitis earlier and at lower doses than the C57BL/6J, making these strains good models for studies evaluating early radiation induced pneumonitis; however, these strains do not typically develop pulmonary fibrosis and are therefore poor models for the evaluation the full progression of radiation induced lung injury.[1]

Although the pathogenesis in mice appears to be similar to humans and NHPs, their small

size historically required irradiation of the entire thorax, which does not typically correlate with the clinical application of targeted small field RT in human patients. This limitation necessitated the use of larger animal models such as pigs and NHPs to allow for hemi-thorax or smaller targeted fields. However, the recent advent of small animal irradiators has provided researchers with the ability to replicate small field RT in murine models.[1]

Differentials of similar lesions in various species proposed by the moderator include direct (i.e. inhaled) toxins such as oxygen, ozone, nitrous dioxide, and smoke; indirect toxins such as paraquat, 4-ipomeanol, purple mint, stinkwood, rapeseed, and kale; type III hypersensitivity reactions, and potentially infectious etiologies. Conference attendees also noted increased eosinophils in the examined section, for which the underlying cause is unclear, but appears to be a stereotypical inflammatory response in some nonhuman primate species.

References:

1. Beach TA, Groves AM, Williams JP, Finkelstein JN. Modeling radiation-induced lung injury: lessons learned from whole thorax irradiation. *Int J Radiat Biol*. 2020;96(1):129-144.
2. Cline JM, Dugan G, Bourland JD, et al. Post-Irradiation Treatment with a Superoxide Dismutase Mimic, MnTnHex-2-PyP5+, Mitigates Radiation Injury in the Lungs of Non-Human Primates after Whole-Thorax Exposure to Ionizing Radiation. *Antioxidants (Basel, Switzerland)*. 2018;7(3):40.
3. Coggle JE, Lambert BE, Moores SR. Radiation effects in the lung. *Environ Health Perspect*. 1986;70:261-291.
4. Duru N, Wolfson B, Zhou Q. Mechanisms of the alternative activation of macrophages and non-coding RNAs in the development of radiation-induced lung fibrosis. *World J Biol Chem*. 2016;7(4):231-239.
5. Epperly M, Bray J, Kraeger S, et al. Prevention of late effects of irradiation lung damage by manganese superoxide dismutase gene therapy. *Gene Ther*. 1998;5(2):196-208.
6. Lombardini, Eric D; Pacheco-Thompson, Michelle E; Melanson MA. Radiation and Other Physical Agents. In: *Haschek and Rousseaux's Handbook of Toxicologic Pathology*. San Diego, United States: Elsevier Science & Technology; 2013.
7. McKenzie E, Razvi Y, Bosnic S, et al. Case series of radiation pneumonitis in breast cancer [published online ahead of print, 2021 Dec 9]. *J Med Imaging Radiat Sci*. 2021;S1939-8654(21)00296-4.
8. Parker GA, Li N, Takayama K, Farese AM, MacVittie TJ. Lung and Heart Injury in a Nonhuman Primate Model of Partial-body Irradiation with Minimal Bone Marrow Sparing: Histopathological Evidence of Lung and Heart Injury. *Health Phys*. 2019;116(3):383-400.
9. Reisz JA, Bansal N, Qian J, Zhao W, Furdui CM. Effects of ionizing radiation on biological molecules--mechanisms of damage and emerging methods of detection. *Antioxid Redox Signal*. 2014;21(2):260-292. doi:10.1089/ars.2013.5489
10. Van Dyk J, Keane TJ, Kan S, Rider WD, Fryer CJ. Radiation pneumonitis following large single dose irradiation: a re-evaluation based on absolute dose to lung. *Int J Radiat Oncol Biol Phys*. 1981;7(4):461-467.